VIP Hollow Nanostructures Very Important Paper

Deutsche Ausgabe: DOI: 10.1002/ange.201606776
Internationale Ausgabe: DOI: 10.1002/anie.201606776

Formation of CoS_2 Nanobubble Hollow Prisms for Highly Reversible Lithium Storage

*Le Yu, Jing Fan Yang, and Xiong Wen (David) Lou**

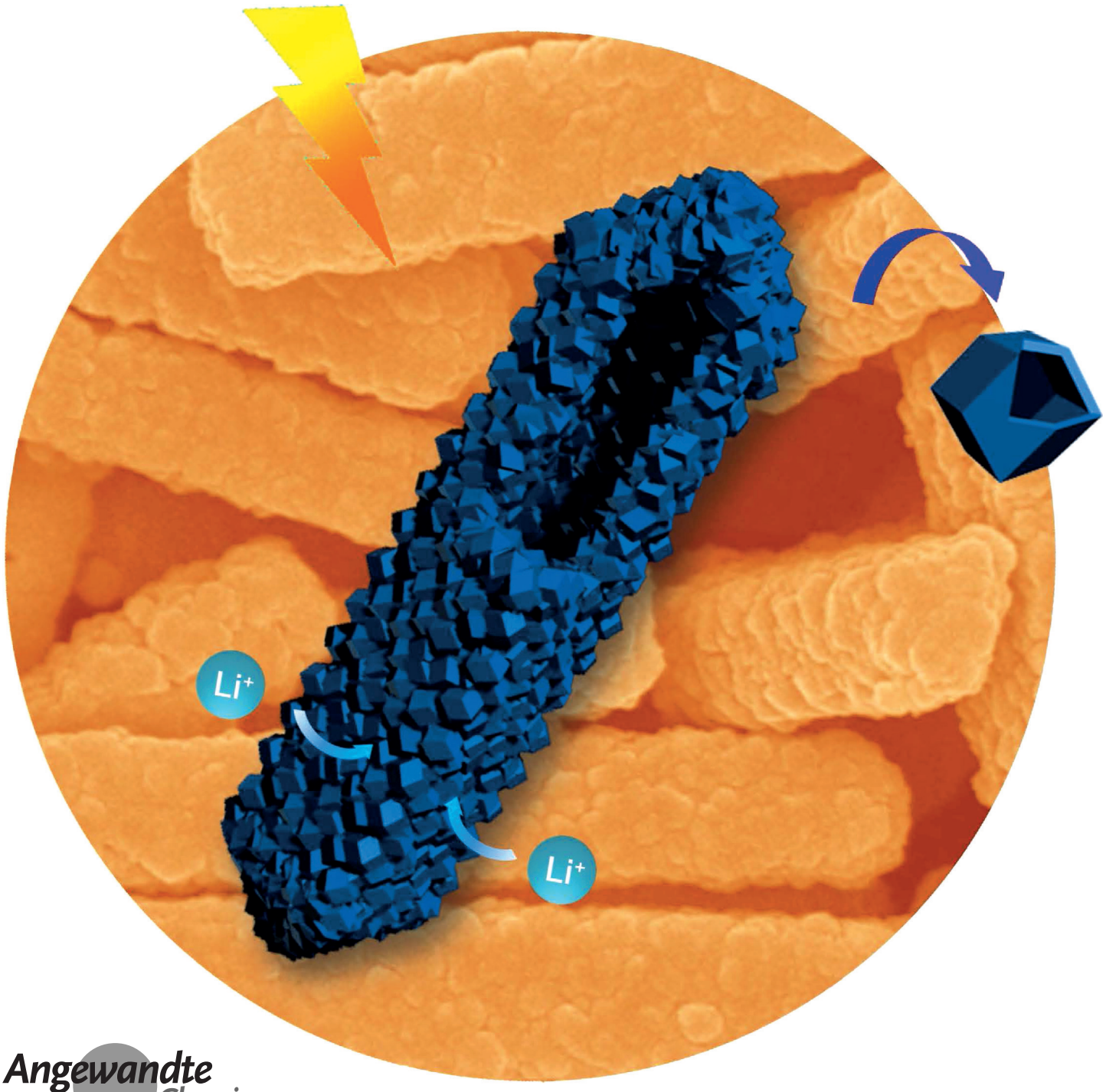

Abstract: *Metal–organic frameworks (MOFs) have been intensively used as the templates/precursors to synthesize complex hollow structures for various energy-related applications. Herein we report a facile two-step diffusion-controlled strategy to generate novel MOFs derived hierarchical hollow prisms composed of Nanosized CoS_2 bubble-like subunits. Uniform zeolitic imidazolate framework-67 (ZIF-67) hollow prisms assembled by interconnected nanopolyhedra are first synthesized via a transformation process. Afterwards, these ZIF-67 building blocks are converted into CoS_2 bubble-like hollow particles to form the complex hollow prisms through a sulfidation reaction with an additional annealing treatment. When evaluated as an electrode material for lithium-ion batteries, the as-obtained CoS_2 nanobubble hollow prisms show remarkable electrochemical performance with good rate capability and long cycle life.*

Lithium-ion batteries (LIBs) are currently the dominant power sources for portable electronic devices, and potentially also for electric vehicles and hybrid electric vehicles.[1–5] Meanwhile, numerous efforts have been devoted to explore new electrode materials to push the power/energy density limit set by the intercalation reactions of electrode materials used in current LIBs. Metal sulfides with their rich redox chemistry, enhanced electrical conductivity, and high capacity, are considered as advanced anode materials compared to the state-of-the-art carbonaceous anodes.[6–9] Owing to the large volume changes associated with the repeated lithium uptake and removal processes, particle fracture and loss of electrical contact have long been identified as primary causes for the capacity fading of metal oxides/sulfides based anodes.[10] The utilization of nanostructures, especially hollow-structured micro-/nanomaterials, offers great promise to mitigate the above-mentioned obstacles and retain the integrity of the electrodes by withstanding the pronounced (de)lithiation strain.[6,10] In particular, complex hollow structures with multilevel internal architectures, such as multi-layered shells or multiple chambers/channels are proved to be highly desirable for lithium storage with their enhanced packing density yet preserving all the advantages of hollow structures.[11–17]

Owing to their diverse structural and compositional functionalities, metal–organic frameworks (MOFs) formed by supramolecular assembly of metal ions with organic struts have been intensively employed as an emerging class of precursors/templates to construct hollow nanostructures with unique architectures in the last few years.[18–25] Very recently, hollow structured MOFs have enabled the generation of hollow architectures with high complexity in the building blocks and compositions.[26–28] For example, Zou et al. reported the synthesis of novel hollow octahedra composed of carbon stabilized $ZnO/ZnFe_2O_4$ nanoparticles by using hollow MOF-5 as both the precursor and self-sacrificing template.[28] A surface-energy-driven mechanism may be responsible for the formation of hollow MOF nanocages.[29] Lou and co-workers have recently prepared Ni–Co Prussian-blue-analogue (PBA) nanocages consisting of pyramidal walls through a direct etching method and the derived cage-like Ni–Co-mixed-oxide samples can well preserve the structural features from the hollow precursors.[27] Despite the progress achieved to date, the construction of nanosized hollow MOFs is still relatively less reported due to the limited morphologies of the MOF precursors.[27,29–36] Therefore, it is highly desirable to explore new synthetic protocols and concepts for the fabrication of hollow MOFs and derived functional nanomaterials.

Herein we report the synthesis of uniform zeolitic imidazolate framework-67 (ZIF-67) prism-like hollow structures transformed from cobalt acetate hydroxide solid precursors. Importantly, these ZIF-67 hollow prisms can be further converted into hollow nanoprisms assembled by nanosized CoS_4 bubble-like subunits by a sulfidation reaction with thioacetamide (TAA) in ethanol. After the thermal treatment under inert atmosphere, the obtained hierarchical CoS_2 hollow prisms manifest remarkable electrochemical performance as an anode material for LIBs with high rate capability and long-term cycling stability.

The synthetic strategy for the CoS_2 nanobubble hollow prisms is schematically depicted in Figure 1 (see Supporting Information for the detailed synthesis). We first develop a fast ion-exchange method to convert the highly uniform cobalt acetate hydroxide nanoprisms into ZIF-67 hollow prisms in ethanol solution of 2-methylimidazole. The evolution of hollow interior might be ascribed to the diffusion effect of different cationic and anionic species.[37,38] During the chemical transformation, the outward diffusion of smaller ions from the solid precursors takes the lead for the steady growth of ZIF-67 shells over the whole particle. As a result, a prism-like structure assembled by interconnected ZIF-67 polyhedral particles is formed with the well-defined internal void. A subsequent sulfidation reaction is carried out to convert the ZIF-67 subunits into CoS_4 bubble-like particles. In this step,

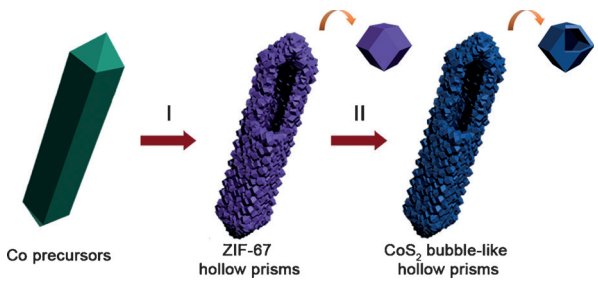

Figure 1. Schematic illustration on the formation of CoS_2 nanobubble hollow prisms via a two-step self-templating strategy. I) The formation of ZIF-67 hollow prisms through a diffusion-controlled process. II) The sulfidation reaction and subsequent thermal treatment to generate hollow prisms formed of CoS_2 nanobubbles.

[*] Dr. L. Yu, J. F. Yang, Prof. X. W. Lou
School of Chemical and Biomedical Engineering
Nanyang Technological University
62 Nanyang Drive, Singapore 637459 (Singapore)
E-mail: xwlou@ntu.edu.sg
davidlou88@gmail.com
Homepage: http://www.ntu.edu.sg/home/xwlou/

Supporting information for this article can be found under: http://dx.doi.org/10.1002/anie.201606776.

the hollowing strategy for the building units can also be described as a diffusion-controlled ion exchange process, which is widely employed to create a central void for metal sulfide nanostructures.[6,37] After a thermal treatment in nitrogen, crystalline hierarchical CoS_2 prisms with multilevel hollow interiors are obtained.

High-aspect-ratio cobalt acetate hydroxide prisms (denoted as Co precursors) are first prepared via a modified precipitation method and applied as the self-engaged templates. The morphological observations (Figure S1, Supporting Information) indicate the solid nature of these highly uniform Co precursors with smooth surface over the whole particle. The corresponding X-ray diffraction (XRD; Figure S2, Supporting Information) pattern confirms that the crystalline Co precursors have a tetragonal cobalt acetate hydroxide phase without any impurities.[39] After the transformation of the prism precursors in the presence of 2-methylimidazole, all the identified diffraction peaks (Figure S3, Supporting Information) of resultant particles can be assigned to the ZIF-67 phase without noticeable signals of residues. The energy-dispersive spectroscopy (EDX) spectrum (Figure S4, Supporting Information) verifies the existence of N and C elements from the organic ligand. Figure 2

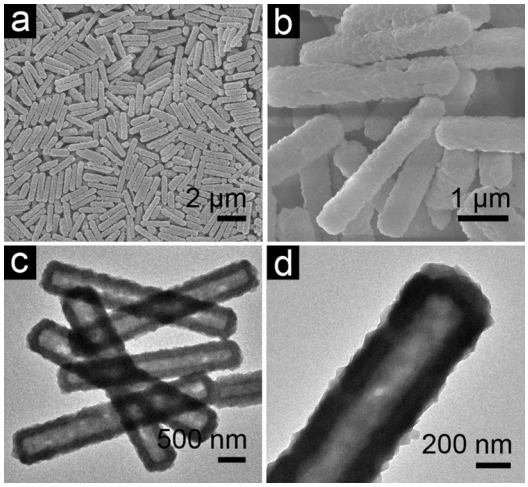

Figure 2. a),b) FESEM and c),d) TEM images of ZIF-67 hollow prisms.

shows the typical morphology and microstructure of the as-prepared ZIF-67 samples. The corresponding panoramic field-emission scanning electron microscopy (FESEM) image (Figure 2a) reveals that the overall prism-like appearance is well inherited without significant alternations. From the increased surface roughness shown in the magnified image (Figure 2b), it can be deduced that these Co precursors are successfully transformed into ZIF-67 prisms constructed by numerous interconnected subunits. The transmission electron microscopy (TEM) image (Figure 2c) clearly elucidates the hollow nature of the ZIF-67 prisms by the sharp contrast between the grained shell and the central void space. As shown by the partially enlarged TEM image (Figure 2d), the thickness of ZIF-67 wall is about 120 nm.

During the morphology evolution of these hierarchical hollow prisms, ZIF-67 subunits are uniformly grown on the surface of prisms at the expense of the solid Co precursors (Figure S5, Supporting Information). It is worth mentioning that the amount of 2-methylimidazole plays a significant role on the morphologies of the ZIF-67 hollow prisms. When the amount of organic ligand added is insufficient, only some small ZIF-67 particles are formed around the surface of the Co precursors (Figure S6a, Supporting Information). On the contrary, the excess dosage of reactant will lead to the overgrowth of polyhedral subunits and destruction of the prism shape (Figure S6b, Supporting Information). Moreover, the choice of solvent is also very critical to obtain the desirable ZIF-67 structure. For example, the use of methanol will favor the homogeneous formation of ZIF-67 particles in the solution (Figure S7a, Supporting Information). Whereas the particles obtained in isopropanol are not robust enough to retain the original prism-like shape (Figure S7b, Supporting Information).

The as-prepared ZIF-67 hollow prisms can withstand the sulfidation treatment in TAA solution with the mild reaction conditions. As seen from the FESEM image (Figure 3a), the

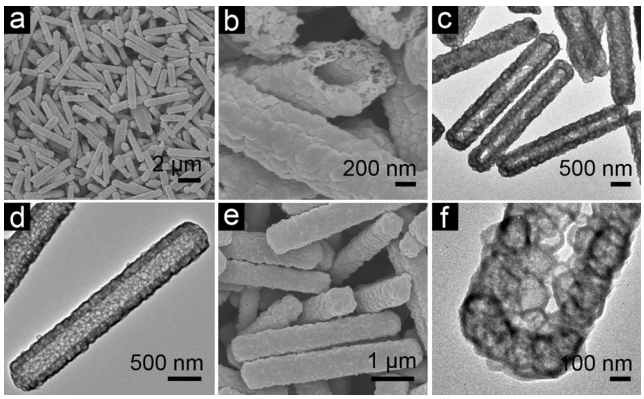

Figure 3. a),b) FESEM and c),d) TEM images of CoS_4 nanobubble hollow prisms obtained after sulfidation in ethanol. e) FESEM and f) TEM images of CoS_2 nanobubble hollow prisms obtained after annealing in nitrogen at 350°C.

derived particles can retain the structural features of precursors. The complete phase conversion is corroborated by XRD analysis (Figure S8, Supporting Information) with low-intensity broad peaks, revealing the very small size of sulfide nanocrystallites. The EDX result (Figure S9, Supporting Information) reveals a Co/S atomic ratio of about 0.23, indicating the formed products might be CoS_4. From a broken prism shown in Figure 3b, the hollow interior and the primary nanometer-sized bubble-like building units can be clearly discerned. TEM images (Figure 3c,d) further elaborate the multilevel hollow interiors of the CoS_4 prisms. Intriguingly, the shell of hollow prisms is composed of interlinked nanobubbles with ultrathin shell thickness. It is obvious that each CoS_4 nanobubble has evolved from one individual ZIF-67 subunit during the conversion process. From the XRD pattern (Figure S10, Supporting Information), the crystallinity of the sulfide samples increases significantly after thermal anneal-

ing. All the Bragg peaks can be approximately indexed to the CoS_2 phase (JCPDS card No. 41–1471). The elemental composition analysis (Figure S11, Supporting Information) reveals a Co/S atomic ratio of 0.51, confirming the dominant CoS_2 phase. As shown in the FESEM image (Figure 3e), the particles exhibit no apparent structural change after the annealing process. A closer TEM examination of an individual CoS_2 prism (Figure 3f) further confirms these peculiar hollow structures are composed of many interconnected bubble-like polyhedra with a shell thickness of 20–30 nm.

As determined by N_2 sorption measurement (Figure S12, Supporting Information), these hierarchical CoS_2 hollow prisms possess a Brunauer-Emmett-Teller (BET) specific surface area of 28.1 $m^2 g^{-1}$ with a pore volume of 0.07 $cm^3 g^{-1}$. The corresponding pore size distribution curve shows the size of majority of these pores is in the range of 2–10 nm.

Next, we evaluate the electrochemical properties of as-obtained CoS_2 hollow prisms as an anode material for LIBs. Figure 4a presents the typical galvanostatic charge-discharge voltage profiles at a current density of 200 mA g^{-1} within a cut-off potential range of 0.05–3.0 V versus Li/Li^+. The initial discharge and charge specific capacities are 1542 and 861 mAh g^{-1}, respectively. The large irreversible capacity in the first cycle could result from the incomplete restoration of metallic Co into the original oxidation states, the irreversible loss of the lithium in the formation of the solid-electrolyte interphase (SEI) film and the decomposition of electrolyte.[40,41] To further study the mechanism of lithium storage in this CoS_2 electrode, the differential chronopotentiometric curves calculated from the charge-discharge data (Figure S13, Supporting Information) are carefully investigated. In the first discharge process, three pronounced peaks around 0.6, 0.9 and 1.3 V are observed. Meanwhile, from the second cycle onwards, only two reversible peaks centered at 0.7 and 1.7 V can be found. The clear changes of the peak number and position shift reveal the different redox behaviors, which might be ascribed to the irreversible side reactions and some possible activation process caused by the initial lithium insertion in the first cycle.[6,40–43] As for the charge process, the reproducible peak located around 2.0 V can be attributed to oxidation reaction of Co nanocrystals.[40–43]

The rate capability of the electrode is tested through galvanostatic measurements at various current densities (Figure 4b). Despite the slight capacity fading during the initial cycles, the CoS_2 hollow prisms can deliver remarkably high reversible specific capacities of 910, 778, 681, and 470 mAh g^{-1} at the current densities of 200, 500, 1000, and 5000 mA g^{-1}, respectively. Moreover, the capacity quickly recovers to as high as 864 mAh g^{-1} when the current density is finally reduced back to 200 mA g^{-1}, suggesting excellent robustness of the electrode. The long-term cycling performance of the CoS_2 hollow prisms and corresponding Coulombic efficiency at a constant charge–discharge current density of 1000 mA g^{-1} are displayed in Figure 4c. From the second cycle onwards, the discharge capacity quickly stabilizes. The gradual capacity decay in the first 50 cycles might be ascribed to the SEI film stabilization and irreversible trapping of some lithium in the lattice.[44,45] Remarkably, these CoS_2 hollow prisms show excellent cycling performance and eventually deliver a reversible capacity of about 737 mAh g^{-1} after 200 cycles, which is around 85% of the second cycle capacity. The Coulombic efficiency (CE) increases rapidly over the course of first few cycles to almost 100% afterwards. Overall, the lithium storage properties of the CoS_2 hollow prisms are superior to those of many previously reported cobalt sulfide-based electrodes.[25,40,41,44,46] The enhanced electrochemical performance of the hierarchical CoS_2 hollow prisms might be attributed to the unique structural features. Apparently, the primary nanobubbles with ultrathin shells could largely reduce the Li^+ ion diffusion length to improve the electrochemical kinetics. More importantly, the hierarchical prisms composed by these bubble-like subunits offer multilevel hollow interior to effectively accommodate the structural stress during the repeated charge–discharge processes. As a result, the integrity of the electrode is well preserved to ensure the long-term cycling stability as revealed by post-mortem observation (Figure S14, Supporting Information).

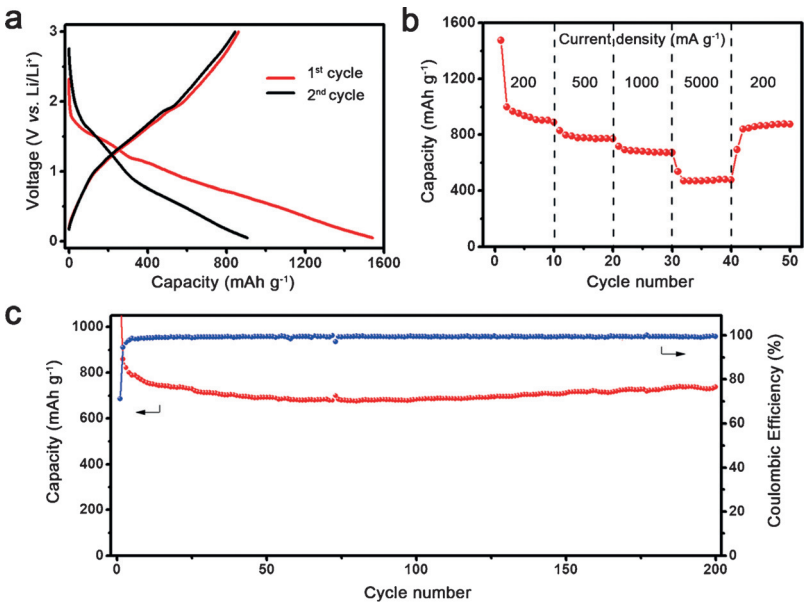

Figure 4. Electrochemical evaluation of the CoS_2 nanobubble hollow prisms electrode. a) Galvanostatic charge–discharge voltage profiles at 200 mA g^{-1}. b) Rate capabilities at various current densities and c) cycling performance at 1000 mA g^{-1} and the corresponding Coulombic efficiency. All measurements were conducted in the voltage range of 0.05–3.0 V versus Li/Li^+.

In summary, we have synthesized novel CoS_2 hollow prisms constructed by interconnected bubble-like subunits by a facile two-step self-engaged method. Prism-like cobalt acetate hydroxide particles are first transformed into hollow prisms composed of ZIF-67 crystals, which are then converted into CoS_4 hollow prisms composed of bubble-like subunits. The hollowing mechanisms involved in both steps can be described by diffusion-controlled processes. Benefiting from the

structural advantages, the final hierarchical CoS_2 hollow prisms have enhanced electrochemical performance as an anode material for lithium-ion batteries. Specifically, these CoS_2 hollow prisms deliver high specific capacities with desirable capacity retention over 200 cycles.

Acknowledgements

X.W.L. is grateful to the Ministry of Education (Singapore) for financial support through the AcRF Tier 2 funding (MOE2014-T2-1-058, ARC41/14; M4020223.120).

Keywords: CoS_2 · hollow prisms · lithium-ion batteries · ZIF-67

How to cite: *Angew. Chem. Int. Ed.* **2016**, *55*, 13422–13426
Angew. Chem. **2016**, *128*, 13620–13624

[1] M. Armand, J. M. Tarascon, *Nature* **2008**, *451*, 652–657.
[2] K. S. Kang, Y. S. Meng, J. Breger, C. P. Grey, G. Ceder, *Science* **2006**, *311*, 977–980.
[3] Y. Idota, T. Kubota, A. Matsufuji, Y. Maekawa, T. Miyasaka, *Science* **1997**, *276*, 1395–1397.
[4] A. Kushima, X. H. Liu, G. Zhu, Z. L. Wang, J. Y. Huang, J. Li, *Nano Lett.* **2011**, *11*, 4535–4541.
[5] H. Jiang, D. Ren, H. Wang, Y. Hu, S. Guo, H. Yuan, P. Hu, L. Zhang, C. Li, *Adv. Mater.* **2015**, *27*, 3687–3695.
[6] X. Y. Yu, L. Yu, X. W. Lou, *Adv. Energy Mater.* **2016**, *6*, 1501333.
[7] X. Xu, W. Liu, Y. Kim, J. Cho, *Nano Today* **2014**, *9*, 604–630.
[8] M. R. Gao, Y. F. Xu, J. Jiang, S. H. Yu, *Chem. Soc. Rev.* **2013**, *42*, 2986–3017.
[9] X. Huang, Z. Y. Zeng, H. Zhang, *Chem. Soc. Rev.* **2013**, *42*, 1934–1946.
[10] C. Liu, F. Li, L. P. Ma, H. M. Cheng, *Adv. Mater.* **2010**, *22*, E28–E62.
[11] J. Qi, X. Y. Lai, J. Y. Wang, H. J. Tang, H. Ren, Y. Yang, Q. Jin, L. J. Zhang, R. B. Yu, G. H. Ma, Z. G. Su, H. J. Zhao, D. Wang, *Chem. Soc. Rev.* **2015**, *44*, 6749–6773.
[12] Z. Li, J. T. Zhang, Y. M. Chen, J. Li, X. W. Lou, *Nat. Commun.* **2015**, *6*, 8850.
[13] X. L. Li, M. Gu, S. Y. Hu, R. Kennard, P. F. Yan, X. L. Chen, C. M. Wang, M. J. Sailor, J. G. Zhang, J. Liu, *Nat. Commun.* **2014**, *5*, 4105.
[14] F. Pei, T. An, J. Zang, X. Zhao, X. Fang, M. Zheng, Q. Dong, N. Zheng, *Adv. Energy Mater.* **2016**, *6*, 1502539.
[15] J. Y. Wang, N. L. Yang, H. J. Tang, Z. H. Dong, Q. Jin, M. Yang, D. Kisailus, H. J. Zhao, Z. Y. Tang, D. Wang, *Angew. Chem. Int. Ed.* **2013**, *52*, 6417–6420; *Angew. Chem.* **2013**, *125*, 6545–6548.
[16] S. M. Xu, C. M. Hessel, H. Ren, R. B. Yu, Q. Jin, M. Yang, H. J. Zhao, D. Wang, *Energy Environ. Sci.* **2014**, *7*, 632–637.
[17] J. Y. Wang, H. J. Tang, L. J. Zhang, H. Ren, R. B. Yu, Q. Jin, J. Qi, D. Mao, M. Yang, Y. Wang, P. Liu, Y. Zhang, Y. R. Wen, L. Gu, G. H. Ma, Z. G. Su, Z. Y. Tang, H. J. Zhao, D. Wang, *Nat. Energy* **2016**, *1*, 16050.
[18] J. T. Zhang, H. Hu, Z. Li, X. W. Lou, *Angew. Chem. Int. Ed.* **2016**, *55*, 3982–3986; *Angew. Chem.* **2016**, *128*, 4050–4054.
[19] B. Y. Xia, Y. Yan, N. Li, H. B. Wu, X. W. Lou, X. Wang, *Nat. Energy* **2016**, *1*, 15006.
[20] H. Hu, L. Han, M. Z. Yu, Z. Y. Wang, X. W. Lou, *Energy Environ. Sci.* **2016**, *9*, 107–111.
[21] X. J. Cai, W. Gao, M. Ma, M. Y. Wu, L. L. Zhang, Y. Y. Zheng, H. R. Chen, J. L. Shi, *Adv. Mater.* **2015**, *27*, 6382–6389.
[22] L. Hu, Q. W. Chen, *Nanoscale* **2014**, *6*, 1236–1257.
[23] L. Zhang, H. B. Wu, X. W. Lou, *J. Am. Chem. Soc.* **2013**, *135*, 10664–10672.
[24] J. Liu, C. Wu, D. D. Xiao, P. Kopold, L. Gu, P. A. van Aken, J. Maier, Y. Yu, *Small* **2016**, *12*, 2354–2364.
[25] R. B. Wu, D. P. Wang, X. H. Rui, B. Liu, K. Zhou, A. W. K. Law, Q. Y. Yan, J. Wei, Z. Chen, *Adv. Mater.* **2015**, *27*, 3038–3044.
[26] Y. M. Chen, L. Yu, X. W. Lou, *Angew. Chem. Int. Ed.* **2016**, *55*, 5990–5993; *Angew. Chem.* **2016**, *128*, 6094–6097.
[27] L. Han, X. Y. Yu, X. W. Lou, *Adv. Mater.* **2016**, *28*, 4601–4605.
[28] F. Zou, X. L. Hu, Z. Li, L. Qie, C. C. Hu, R. Zeng, Y. Jiang, Y. H. Huang, *Adv. Mater.* **2014**, *26*, 6622–6628.
[29] Z. C. Zhang, Y. F. Chen, X. B. Xu, J. C. Zhang, G. L. Xiang, W. He, X. Wang, *Angew. Chem. Int. Ed.* **2014**, *53*, 429–433; *Angew. Chem.* **2014**, *126*, 439–443.
[30] C. Y. Dai, A. F. Zhang, M. Liu, X. W. Guo, C. S. Song, *Adv. Funct. Mater.* **2015**, *25*, 7479–7487.
[31] X. B. Xu, Z. C. Zhang, X. Wang, *Adv. Mater.* **2015**, *27*, 5365–5371.
[32] J. Yang, F. J. Zhang, H. Y. Lu, X. Hong, H. L. Jiang, Y. Wu, Y. D. Li, *Angew. Chem. Int. Ed.* **2015**, *54*, 10889–10893; *Angew. Chem.* **2015**, *127*, 11039–11043.
[33] C. Avci, J. Arinez-Soriano, A. Carne-Sanchez, V. Guillerm, C. Carbonell, I. Imaz, D. Maspoch, *Angew. Chem. Int. Ed.* **2015**, *54*, 14417–14421; *Angew. Chem.* **2015**, *127*, 14625–14629.
[34] M. Hu, S. Furukawa, R. Ohtani, H. Sukegawa, Y. Nemoto, J. Reboul, S. Kitagawa, Y. Yamauchi, *Angew. Chem. Int. Ed.* **2012**, *51*, 984–988; *Angew. Chem.* **2012**, *124*, 1008–1012.
[35] F. Zhang, Y. Y. Wei, X. T. Wu, H. Y. Jiang, W. Wang, H. X. Li, *J. Am. Chem. Soc.* **2014**, *136*, 13963–13966.
[36] M. L. Pang, A. J. Cairns, Y. L. Liu, Y. Belmabkhout, H. C. Zeng, M. Eddaoudi, *J. Am. Chem. Soc.* **2013**, *135*, 10234–10237.
[37] S. L. Xiong, H. C. Zeng, *Angew. Chem. Int. Ed.* **2012**, *51*, 949–952; *Angew. Chem.* **2012**, *124*, 973–976.
[38] L. Yu, L. Zhang, H. B. Wu, X. W. Lou, *Angew. Chem. Int. Ed.* **2014**, *53*, 3711–3714; *Angew. Chem.* **2014**, *126*, 3785–3788.
[39] L. Yu, B. Y. Xia, X. Wang, X. W. Lou, *Adv. Mater.* **2016**, *28*, 92–97.
[40] R. C. Jin, L. X. Yang, G. H. Li, G. Chen, *J. Mater. Chem. A* **2015**, *3*, 10677–10680.
[41] Q. F. Wang, R. Q. Zou, W. Xia, J. Ma, B. Qiu, A. Mahmood, R. Zhao, Y. Y. C. Yang, D. G. Xia, Q. Xu, *Small* **2015**, *11*, 2511–2517.
[42] Q. H. Wang, L. F. Jiao, Y. Han, H. M. Du, W. X. Peng, Q. N. Huan, D. W. Song, Y. C. Si, Y. J. Wang, H. T. Yuan, *J. Phys. Chem. C* **2011**, *115*, 8300–8304.
[43] J. Xie, S. Y. Liu, G. S. Cao, T. J. Zhu, X. B. Zhao, *Nano Energy* **2013**, *2*, 49–56.
[44] Y. L. Zhou, D. Yan, H. Y. Xu, J. K. Feng, X. L. Jiang, J. Yue, J. Yang, Y. T. Qian, *Nano Energy* **2015**, *12*, 528–537.
[45] Z. Y. Wang, Z. C. Wang, W. T. Liu, W. Xiao, X. W. Lou, *Energy Environ. Sci.* **2013**, *6*, 87–91.
[46] P. Sennu, M. Christy, V. Aravindan, Y. G. Lee, K. S. Nahm, Y. S. Lee, *Chem. Mater.* **2015**, *27*, 5726–5735.

Received: July 13, 2016
Published online: August 16, 2016

